Physics Letters A 167 (1992) 185–190
North-Holland

PHYSICS LETTERS A

Regular and chaotic behavior in the new Lorenz system

C. Masoller, A.C. Sicardi Schifino
Instituto de Fisica de la Facultad de Ciencias, T. Narvaja 1674, Montevideo, Uruguay
and Instituto de Fisica de la Facultad de Ingenieria, J. Herrera y Reissig 565, CC30, Montevideo, Uruguay

and

Lilia Romanelli
Departamento de Fisica, F.C.E. y N. (U.B.A.), Ciudad Universitaria (1428), Buenos Aires, Argentina

Received 21 August 1991; revised manuscript received 11 May 1992; accepted for publication 13 May 1992
Communicated by A.R. Bishop

The new Lorenz system of general circulation of the atmosphere, which exhibits an immense variety of bifurcation sequences, is studied by computer simulation. When the external heating varies, periodic and turbulent regions are found. In the periodic regions, period-doubling, period-halving and saddle-node bifurcations are observed. Also, at certain parameter intervals, hysteresis and coexistence of attractors is reported. The chaotic behavior in the turbulent region is discussed with the aid of Lyapunov analysis and correlation dimension calculations.

In recent years, a great deal of interest has been focused on studying the complexity of nonlinear dynamical systems. Lorenz's classical model of thermal convection in the atmosphere [1] was the first chaotic system discovered and has been one of the most extensively investigated. As a modification of this model of turbulence generation, in refs. [2,3] Lorenz derived a simple but powerful model based on the "general circulation" of the atmosphere. In ref. [3], when the external heating F varies and the heating contrast between oceans and continents G is equal to 1, several attractors were found. The coexistence of two periodic attractors (the "weak" and the "strong" attractors) was determined under summer conditions ($F=6.0$), while only one chaotic attractor was found under winter conditions ($F=8.0$).

The purpose of the present study is to further explore the dynamics of the model when the parameter F is varied. We first study briefly the origin and evolution of the weak and the strong attractors. We show that while the weak attractor is created by a Hopf bifurcation of a stationary solution, the strong attractor appears after a reverse saddle-node bifurcation of the other two fixed points. In addition, we demonstrate that the system's transition to chaos is a Hopf bifurcation where the "weak" limit cycle becomes unstable. Next, we investigate the system's behavior in the turbulent region ($F=8.0$). The Poincaré-section of the attractor presents the typical features of a strange attractor. Moreover, Lyapunov spectrum analysis provides real evidence for chaos since one positive Lyapunov exponent is found. In addition, a correlation dimension of 2.23 was determined.

The model equations are

$$dX/dt=-Y^2-Z^2-aX+aF\,, \tag{1a}$$

$$dY/dt=XY-bXZ-Y+G\,, \tag{1b}$$

$$dZ/dt=bXY+XZ-Z\,, \tag{1c}$$

where the parameter F represents the cross-latitude external-heating contrast, G the heating contrast between oceans and continents, and a and b are positive parameters ($a<1$ and $b>1$). The variable X represents the westerly-wind current and also the poleward temperature gradient which is assumed to be in permanent equilibrium with it, while the variables Y and Z represent the cosine and sine phases of a chain of superposed eddies, which transport heat poleward and can be identified with Rossby waves [2]. In this model t represents the time, and a unit of time is equal to 5 days.

In order to investigate the evolution of the system, we have done a numerical simulation using a standard sixth-order Runge–Kutta integration routine, where the time increment was 0.01 (1.2 h). The parameters were fixed as $a=\frac{1}{4}$, $b=4$, $G=1$ and F varying in the interval [1, 8] as the control parameter. The solution describes a trajectory in the X, Y, Z space. The trajectory obtained after transients have died away constitutes the attractor, which is projected in the (Y, Z) plane.

First, we examine the behavior of the stationary solutions and their linear stability. As fig. 1 shows, the system has one stable fixed point in the region $F<1.188$ (labeled 1). At $F=1.188$ a saddle-node bifurcation occurs and two new fixed points are born: one unstable (labeled 2) and one stable (labeled 3). The initially stable focus 3 becomes unstable at $F=1.27$ after a Hopf bifurcation, and a limit cycle (the "weak" limit cycle) appears. In addition, at $F=4.31$ a reverse saddle-node bifurcation occurs when points 1 (sink) and 2 (saddle) collide and disappear completely. After this crisis, a new periodic orbit appears (the "strong" limit cycle) as a consequence of global changes in the phase portrait [4].

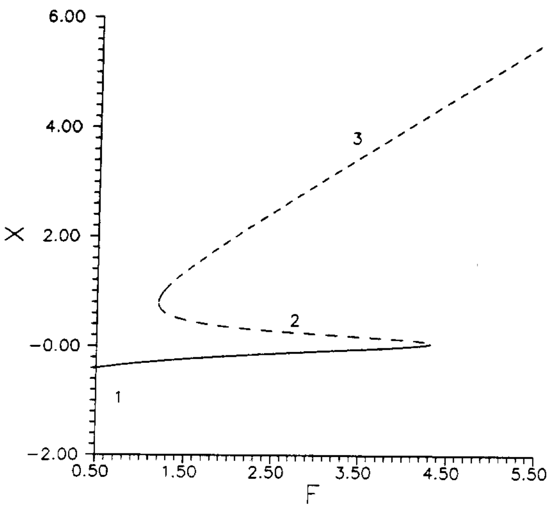

Fig. 1. Coordinate X of the fixed points as a function of F. In the regions $F<1.18$ and $F>4.31$ there is a single fixed point (a sink and a saddle, respectively), while in the region $1.18<F<1.27$ there are two sinks and one saddle and in the region $1.27<F<4.31$ there are one sink and two saddles.

The weak and the strong limit cycles are clearly different from each other (see figs. 2 and 3). The weak limit cycle has a smaller amplitude and a much shorter period than the strong limit cycle. Moreover, the convergence to the weak limit cycle is weaker, i.e., nearby points are attracted to it relatively slowly.

Let us now investigate the evolution of these limit cycles. For the location of a periodic orbit, an ex-

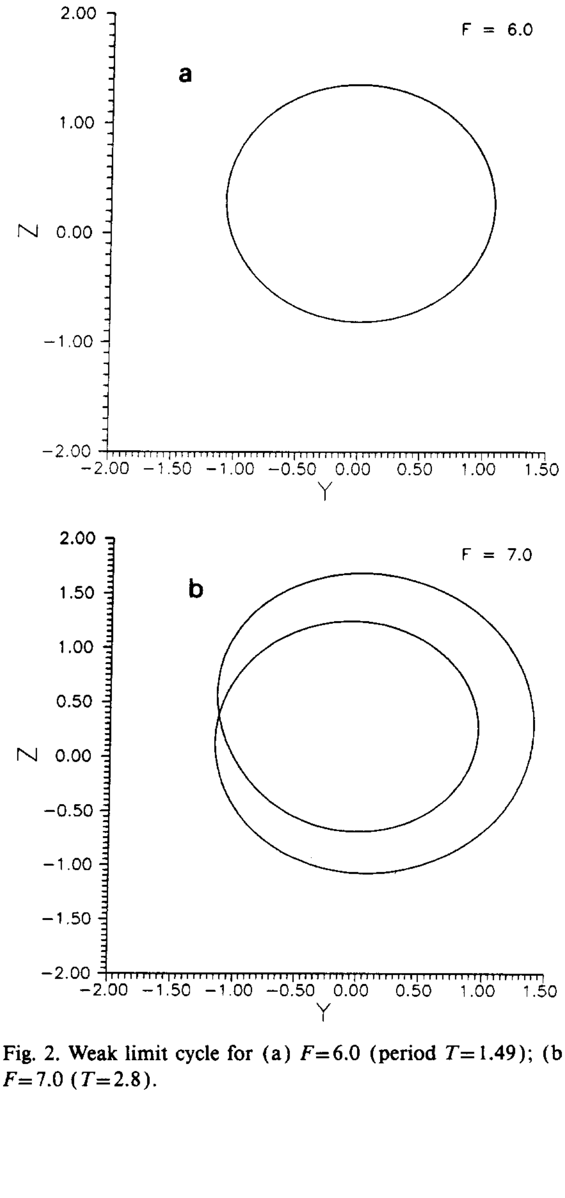

Fig. 2. Weak limit cycle for (a) $F=6.0$ (period $T=1.49$); (b) $F=7.0$ ($T=2.8$).

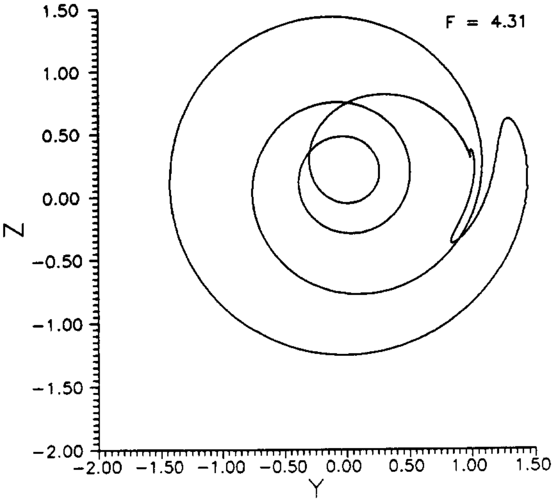

Fig. 3. Strong limit cycle for $F=4.31$ (period $T=56.27$).

tension of Newton's method of tangents [5] was used. Once we located a limit cycle, its stability was studied calculating the eigenvalue spectrum of the linearized Poincaré map (Floquet matrix [4,6]). These eigenvalues λ_1, λ_2, λ_3 are the characteristic multipliers of the limit cycle. The multiplier associated with a perturbation along the orbit is always unity (let this be λ_3), while the remaining two determine the stability of the orbit. A periodic orbit is linearly stable if its multipliers are <1 in modulus, and unstable if at least one multiplier is >1 in modulus. Let us now describe briefly the results obtained.

As we have said, the weak attractor (shown in fig. 2) is born after a (supercritical) Hopf bifurcation of focus 3. The amplitude of the limit cycle smoothly increases while its period slowly decreases as the parameter F is increased. This limit cycle undergoes a period-doubling bifurcation at $F=6.25$ when one eigenvalue traverses the unit circle in -1, and at $F=7.85$ loses stability after a Hopf bifurcation, where two complex conjugated eigenvalues simultaneously cross the unit circle at about -0.76 ± 0.61.

Above $F=7.85$, a strange attractor appears (illustrated in fig. 4). We shall call this region the turbulent region. Hysteresis is exhibited near the Hopf bifurcation since the chaotic attractor is barely unstable, i.e., close to the bifurcation point, trajectories originated near the weak limit cycle remain close to it, while trajectories originated far from it, evolve chaotically for a while before arriving near the pe-

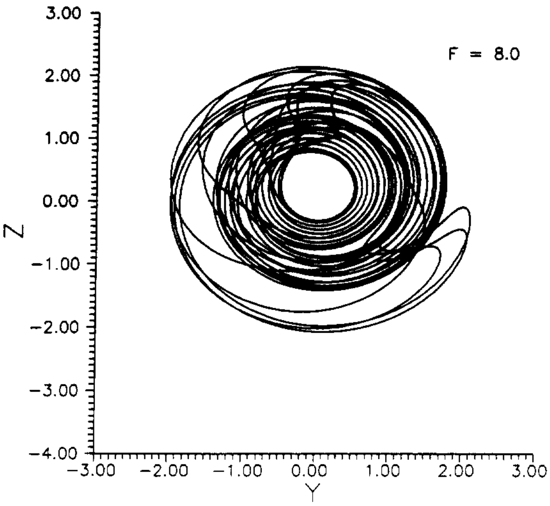

Fig. 4. Projection of a part of a trajectory onto the plane (Y, Z) in the turbulent region ($F=8.0$).

riodic orbit, where they converge rapidly.

As was mentioned before, the strong limit cycle (shown in fig. 3) is born after the reverse saddle-node bifurcation of the stationary solutions 1 and 2. Contrary to the weak limit cycle, the strong limit cycle displays remarkably complex dynamics. As F is varied, several periodic regimes appear ("windows of periodicity"). These windows are the domains of different strong limit cycles, and their appearance and disappearance follow the same sequence of events, which we will describe in detail.

The first window begins when the strong limit cycle is born (we shall call this limit cycle cycle A). As F increases, the period of cycle A decreases continuously. At $F=4.48$, a saddle-node bifurcation occurs and a stable (B) and unstable (C) pair of limit cycles appear. Figure 5 shows the coexistence of cycles A, B and C for $F=4.5$.

While cycle A is always stable and cycle C is always unstable (the multipliers are $0<\lambda_1<1<\lambda_2$), cycle B is stable at the beginning but at $F=4.484$ becomes unstable (one eigenvalue crosses the unit circle at -1 and the multipliers are $\lambda_1<-1<\lambda_2<0$). As a consequence a period-doubling bifurcation occurs in which another limit cycle (cycle D) of twice the period appears.

Increasing F, a reverse saddle-node bifurcation occurs when cycles A and C collide and disappear com-

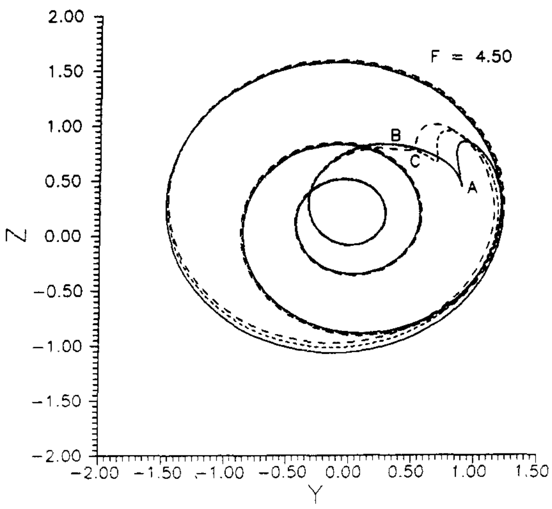

Fig. 5. Coexistence of cycles A, B and C for $F=4.5$.

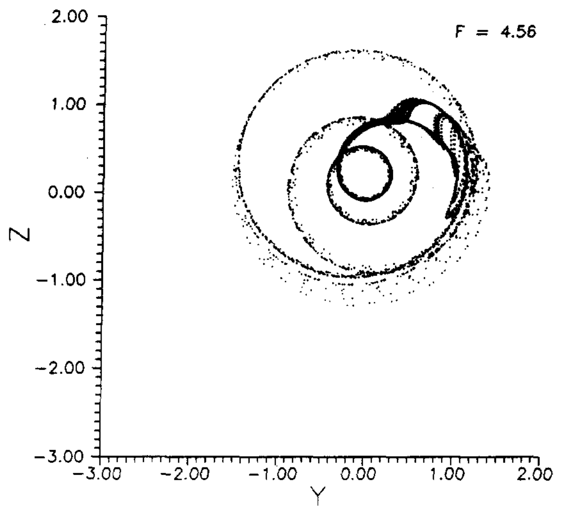

Fig. 6. Chaotic attractor for $F=4.56$.

pletely (at $F=4.52$). After this crisis, a new cycle is born (cycle E).

We next follow the evolution of the limit cycles D and E. Cycle D quickly becomes unstable, when the biggest (in modulus) eigenvalue crosses the unit circle in -1. On the contrary, cycle E suffers a complicated cascade of bifurcations that lead to the chaotic attractor shown in fig. 6. This attractor disappears at $F=4.561$ when a saddle-node bifurcation occurs and two new limit cycles appear (cycles F and G).

This is the beginning of a new window of periodicity. Limit cycle D regains its stability at $F=4.5679$ when the biggest (in modulus) eigenvalue traverses the unit circle in -1. Increasing F, one eigenvalue approaches the value $+1$ until $F=4.5681$ when the limit cycle collides with the unstable cycle F. Above this value of F, the behavior is similar to the one studied before: the creation and annihilation of a stable and unstable pair of limit cycles. In addition, we observe the coexistence of two stable limit cycles in narrow regions of the parameter F. Also, several sequences of period-doubling bifurcations occur. Finally, this periodic window ends when the basic cycle loses stability. The system will then evolve toward the weak limit cycle, which is the only stable attractor that we found in this parameter region.

The next window begins at $F=5.03$, when another pair of strong limit cycles is born (cycles N, P). A subharmonic cascade arises as the initially stable cycle N becomes unstable at $F=5.062$ due to the passage through -1 of one of the eigenvalues of its Floquet matrix. These period-doubling bifurcations accumulate at a point at which chaotic nonperiodic motion occurs. Increasing F, the diagram of solutions becomes extremely complex. There are some narrow periodic windows appearing within the chaotic regimes and in these periodic windows, period-doubling bifurcations are observed. This behavior is strongly reminiscent of the behavior of the logistic map [7,8].

As F continues to increase, the system shows period-halving or reverse period-doubling bifurcations. This second cascade appears as a consequence of the limit cycle N regaining its stability at $F=5.342$ when one eigenvalue traverses the unit circle in -1. A similar kind of process occurs when the basic limit cycle N again loses stability at $F=6.64$ and regains it at $F=7.45$.

Finally, this periodic window ends at $F=7.5$ when cycle N collides with an unstable limit cycle (Q) and both cycles disappear completely. This unstable limit cycle was born at $F=4.18$ with a stable limit cycle (R). Above this crisis, long chaotic transients appear before the system reaches the "weak" limit cycle, and as was already mentioned, these chaotic transients become stable in the turbulent region, after the weak limit cycle loses stability. In this region, the trajectories projected onto the (Y, Z) plane (see fig. 4) exhibit the irregular appearance of chaotic behavior. It is worthwhile to mention that the coordinates of the unstable fixed point of the flow (focus 3) in this region are approximately $(F, 0, 0)$ and thus the strange attractor shown in fig. 4 is not close to the unstable fixed point.

We observed that the strange attractor exists in a large interval of the parameter F. However, higher values of F give rise to simple periodic motions of small period again. The transition between these two motions and the behavior of the system for higher values of F will be discussed elsewhere.

We now turn to study the dynamics in the turbulent region ($F=8.0$). In order to visualize the dynamics in the turbulent region we pick the cross section $\{(x, y, z)/z=0\}$ and consider the Poincaré map shown in fig. 7. Note that the irregular motion of fig. 4 displays considerable structure when viewed in a Poincaré map, and that it appears to be truly aperiodic. Also, note the self-similarity (Cantor-set) structure of this map, characteristic of strange attractors.

In order to arrive at a deeper understanding of the dynamics, we now turn to the calculation of the Lyapunov exponents and correlation dimension of the attractor.

Lyapunov exponents provide the best quantitative measure of chaotic behavior by describing the mean

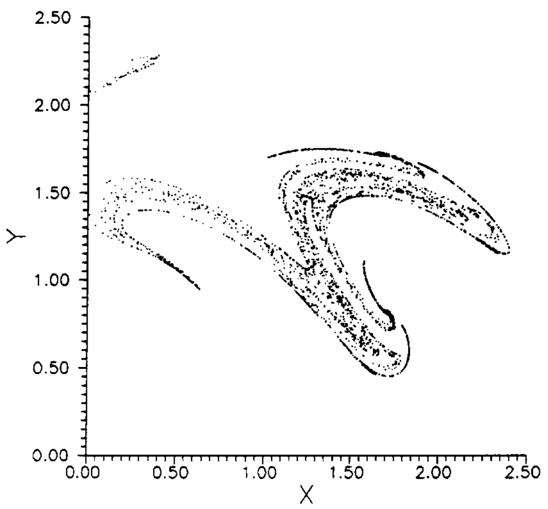

Fig. 7. Poincaré map of the strange attractor of fig. 4.

rate of exponential divergence of initially neighboring trajectories. We have calculated the complete Lyapunov spectrum using the method proposed by Wolf et al. [9]. The resulting Lyapunov exponents (0.23, 0, −0.59) clearly indicate that the system's dynamics is chaotic (power spectrum also supports this conclusion). The reciprocal of the positive exponent provides the characteristic time scale to practical prediction (21 days). Also, note the hyperbolic nature of this attractor, with stronger convergence of trajectories in one direction than divergence in another.

Strange attractors are typically characterized by a fractal dimension. The method proposed by Grassberger and Procaccia [10] leads to the determination of the correlation dimension D_2 which is a lower bound of the Hausdorff dimension. The correlation dimension was calculated from the three-dimensional time series $\{X_i(t), Y_i(t), Z_i(t)\}$ using 70000 data points and a value of $D_c=2.23$ was found.

It is worthwhile to mention that when $G=0$ the system is symmetric under the transformation $(X, Y, Z)\to(X, -Y, -Z)$ and as a consequence we can rewrite eqs. (1) as

$$\mathrm{d}x/\mathrm{d}t=-m-ax+aF,$$
$$\mathrm{d}m/\mathrm{d}t=2m(x-1), \tag{2}$$

where $x=X$ and $m=Y^2+Z^2$. The points ($x=F$, $m=0$) and ($x=1$, $m=a(F-1)$) are the fixed points of the system. The first point (that is stable if $F<1$) corresponds to the steady state solution $X=F$, $Y=Z=0$, while the second point (that exists and is stable if $F>1$) corresponds to the weak limit cycle $X=1$, $Y^2+Z^2=a(F-1)$. Thus, in the symmetric case only the weak attractor exist and the richness of attractors and complex behavior discussed above does not exist, i.e., the asymmetry between the oceans and the continents plays a fundamental role in the dynamics of the atmosphere.

In summary, we have performed a detailed investigation of the chaotic phenomena in the new Lorenz systems. We have found period-doubling bifurcations to chaos, crisis, reverse period doubling, periodic windows, hysteresis and coexistence of periodic attractors. Finally, the chaotic behavior was discussed with the aid of Poincaré-section, Lyapunov spectrum and correlation dimension analysis.

We acknowledge support from the Programa de Desarrollo de Ciencias Basicas, PEDECIBA (Project URU/84/002-UNDP).

References

[1] E.N. Lorenz, J. Atmos. Sci. 20 (1963) 130.
[2] E.N. Lorenz, Tellus 42A (1990) 378.
[3] E.N. Lorenz, Tellus 36A (1984) 98.
[4] J. Guckenheimer and P. Holmes, Nonlinear oscillations, dynamical systems, and bifurcations of vector fields (Springer, Berlin, 1983).
[5] C. Sparrow, The Lorenz equations: bifurcations, chaos, and strange attractors (Springer, Berlin, 1982).
[6] P. Berge, Y. Pomeau and C. Vidal, Order within chaos (Wiley, New York, 1984).
[7] M.J. Feigenbaum, J. Stat. Phys. 21 (1979) 69.
[8] P. Collet and J.-P. Eckmann, Iterated maps in the interval as dynamical systems (Birkhauser, Basel, 1980).
[9] A. Wolf, J.B. Swift, H.L. Swinney and A. Vastano, Physica D 16 (1985) 285.
[10] P. Grassberger and I. Procaccia, Phys. Rev. Lett. 50 (1983) 346.